



Title	Valence band offset at Al ₂ O ₃ /In _{0.17} Al _{0.83} N interface formed by atomic layer deposition
Author(s)	Akazawa, M.; Nakano, T.
Citation	Applied Physics Letters, 101(12), 122110 https://doi.org/10.1063/1.4754141
Issue Date	2012-09-17
Doc URL	http://hdl.handle.net/2115/50407
Rights	Copyright 2012 American Institute of Physics. This article may be downloaded for personal use only. Any other use requires prior permission of the author and the American Institute of Physics. The following article appeared in Appl. Phys. Lett. 101, 122110 (2012) and may be found at https://dx.doi.org/10.1063/1.4754141
Type	article
File Information	APL101-12_122110.pdf



[Instructions for use](#)

Valence band offset at Al₂O₃/In_{0.17}Al_{0.83}N interface formed by atomic layer deposition

M. Akazawa and T. Nakano

Citation: *Appl. Phys. Lett.* **101**, 122110 (2012); doi: 10.1063/1.4754141

View online: <http://dx.doi.org/10.1063/1.4754141>

View Table of Contents: <http://apl.aip.org/resource/1/APPLAB/v101/i12>

Published by the [American Institute of Physics](#).

Related Articles

An ab-initio study of electronic and optical properties of corundum Al₂O₃ doped with Sc, Y, Zr, and Nb
J. Appl. Phys. **112**, 093709 (2012)

Evidence of Eu²⁺ 4f electrons in the valence band spectra of EuTiO₃ and EuZrO₃
J. Appl. Phys. **112**, 083719 (2012)

Model GW study of the late transition metal monoxides
J. Chem. Phys. **137**, 154110 (2012)

First-principles study of electronic structure and magnetic properties of Cu-doped CeO₂
J. Appl. Phys. **112**, 083702 (2012)

Electronic structure and optical band gap of CoFe₂O₄ thin films
Appl. Phys. Lett. **101**, 161902 (2012)

Additional information on *Appl. Phys. Lett.*

Journal Homepage: <http://apl.aip.org/>

Journal Information: http://apl.aip.org/about/about_the_journal

Top downloads: http://apl.aip.org/features/most_downloaded

Information for Authors: <http://apl.aip.org/authors>

ADVERTISEMENT



Goodfellow
metals • ceramics • polymers • composites
70,000 products
450 different materials
small quantities fast

www.goodfellowusa.com

Valence band offset at $\text{Al}_2\text{O}_3/\text{In}_{0.17}\text{Al}_{0.83}\text{N}$ interface formed by atomic layer deposition

M. Akazawa^{a)} and T. Nakano

Research Center for Integrated Quantum Electronics, Hokkaido University, Sapporo 060-8628, Japan

(Received 10 August 2012; accepted 6 September 2012; published online 21 September 2012)

The valence band offset, ΔE_V , at an $\text{Al}_2\text{O}_3/\text{In}_{0.17}\text{Al}_{0.83}\text{N}$ interface formed by atomic layer deposition was measured by x-ray photoelectron spectroscopy. The conventional method of using the core level separation, ΔE_{CL} , between O 1s and In 4d resulted in $\Delta E_V = 1.3$ eV, which was apparently consistent with the direct observation of the valence band edge varying the photoelectron exit angle, θ . However, ΔE_{CL} and full width at half maximum of core-level spectra were dependent on θ , which indicated significant potential gradients in Al_2O_3 and InAlN layers. An actual ΔE_V of 1.2 eV was obtained considering the potential gradients. © 2012 American Institute of Physics. [<http://dx.doi.org/10.1063/1.4754141>]

Lattice-matched InAlN/GaN heterostructures can provide a two-dimensional electron gas (2DEG) with high density exceeding $2 \times 10^{13} \text{ cm}^{-2}$ (Refs. 1 and 2) owing to the large difference in spontaneous polarization at the interface.³ High-performance InAlN/GaN high-electron-mobility transistors (HEMTs) have been fabricated and reported.^{2,4} To suppress the gate leakage current through the InAlN gate barrier in the application of InAlN/GaN heterostructures to HEMTs, the use of Al_2O_3 to form a metal-insulator-semiconductor (MIS)-gate HEMT has been reported.⁴ In addition, a sufficiently low interface state density at the $\text{Al}_2\text{O}_3/\text{InAlN}$ interface has been reported.⁵ To understand the properties of the $\text{Al}_2\text{O}_3/\text{InAlN}$ interface, the valence band offset, ΔE_V , is an important parameter. However, the measurement of ΔE_V has not been reported for an $\text{Al}_2\text{O}_3/\text{InAlN}$ interface. In this work, we investigated the valence band offset at an $\text{Al}_2\text{O}_3/\text{InAlN}$ interface by x-ray photoelectron spectroscopy (XPS).

Here $\text{Al}_2\text{O}_3/\text{In}_{0.17}\text{Al}_{0.83}\text{N}/\text{GaN}$ structures were prepared and investigated. Undoped $\text{In}_{0.17}\text{Al}_{0.83}\text{N}$ layers were grown on undoped GaN buffer layers on sapphire (0001) substrates by metal-organic vapor phase epitaxy (MOVPE). The In molar fraction of the InAlN layer of 0.17 was confirmed by x-ray diffraction (XRD) measurement. The InAlN surface was treated by hydrofluoric acid prior to Al_2O_3 deposition. The Al_2O_3 layer was deposited by atomic layer deposition (ALD) at 350 °C using H_2O and trimethylaluminum (TMA). Samples with Al_2O_3 layer of 2 nm and 16 nm thickness on the $\text{In}_{0.17}\text{Al}_{0.83}\text{N}$ (15 nm)/GaN (2 μm)/sapphire structure were prepared. The sample with 2-nm-thick Al_2O_3 layer was used for interface investigation, while the other sample was used to extract the bulk material constant of ALD Al_2O_3 . XPS was performed using a monochromated Al- $K\alpha$ x-ray source (1486.6 eV). The binding energy shift induced by the charging of the insulating substrate was calibrated by adjusting the peak position of the C 1s core level to 285.0 eV for each sample surface. If necessary, the photoelectron exit angle, θ (defined as the elevation angle with respect to the sample surface), was changed by tilting the sample to change the photoelectron escape depth, λ , according to

$$\lambda = \lambda_0 \sin \theta, \quad (1)$$

where λ_0 is the inelastic mean free path of photoelectrons.

The O 1s and In 4d spectra from the sample with 2-nm-thick Al_2O_3 observed at $\theta = 45^\circ$ are shown in Fig. 1. We found that the obtained O 1s spectrum consisted of two components as shown by the labels “I” and “II” in Fig. 1(a). These components are referred to as O 1s_I and O 1s_{II} hereafter. The O 1s_{II} component was found to be a surface-related peak that decreased in intensity as θ increased, which was in good agreement with the previous report.⁶ The energy difference between these components was 1.4 eV. It is highly likely

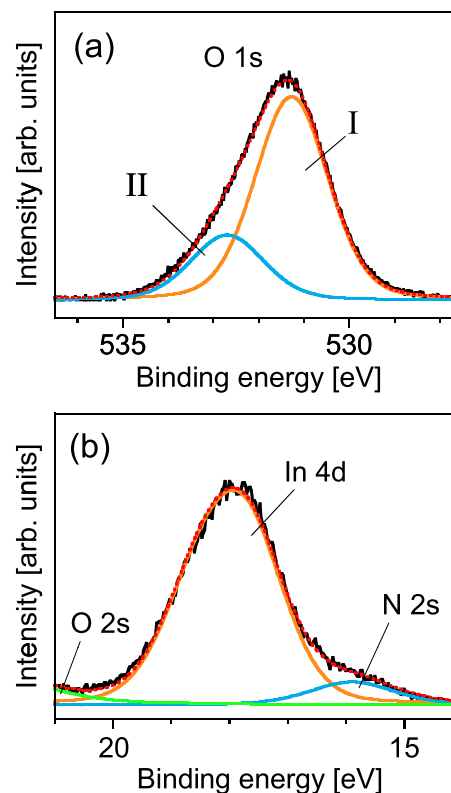


FIG. 1. XPS spectra obtained at $\theta = 45^\circ$ for Al_2O_3 (2 nm)/InAlN interface, (a) O 1s spectrum and (b) In 4d spectrum.

^{a)}Electronic mail: akazawa@rciqe.hokudai.ac.jp.

that the O 1s_I component corresponds to Al-O-Al bonds and the O 1s_{II} component corresponds to Al-O-H bonds, which is in agreement with other reports.^{6,7} In addition, the separation between O 1s_I and the valence band maximum (VBM), E_V , for the 16-nm-thick Al₂O₃ layer was constant and independent of θ , which indicates that this component can be used to determine the bulk constant parameter of the ALD Al₂O₃ layer. Therefore, analysis of the band offset was carried out by using the O 1s_I component.

Using the energy difference between the O 1s_I component and the In 4d spectrum shown in Fig. 1(b), ΔE_V is extracted by the conventional method shown in Fig. 2, where the value of ΔE_V is obtained by the following equation:⁸

$$\Delta E_V = (E_{In4d}^{InAlN} - E_V^{InAlN}) + \Delta E_{CL} - (E_{O1s_I}^{Al_2O_3} - E_V^{Al_2O_3}), \quad (2)$$

where $\Delta E_{CL} = (E_{O1s_I}^{Al_2O_3} - E_{In4d}^{InAlN})$ is the core-level separation between the measured O 1s and In 4d spectra of the Al₂O₃ (2 nm)/In_{0.17}Al_{0.83}N sample. The separations of the core levels from the VBM were found to be $(E_{O1s_I}^{Al_2O_3} - E_V^{Al_2O_3}) = 527.7$ eV and $(E_{In4d}^{InAlN} - E_V^{InAlN}) = 15.7$ eV by measurement of the 16-nm-thick Al₂O₃ and 15-nm-thick InAlN layers. We found that the value of $(E_{O1s_I}^{Al_2O_3} - E_V^{Al_2O_3})$ was constant and independent of θ , while the value of $(E_{In4d}^{InAlN} - E_V^{InAlN})$ was previously obtained by angle resolved-XPS.⁹ The measured core-level separation ΔE_{CL} was 513.3 eV. Consequently, $\Delta E_V = 1.3$ eV was obtained by this conventional method.

This result can be roughly verified by direct measurement of the VBM for the sample with the ultrathin Al₂O₃ layer while changing θ . The VBM of the upper Al₂O₃ layer should be dominant at a sufficiently small θ , whereas that of the lower InAlN layer should appear intensely at a sufficiently large θ . ΔE_V can be roughly obtained by the difference between these VBM, although the precision may be deteriorated by the overlap between two VBM spectra. Figure 3 shows the results for the sample with the 2-nm-thick Al₂O₃ layer used to obtain the data in Fig. 1. As indicated in Fig. 3, the difference in the VBM between $\theta = 15^\circ$ and $\theta = 75^\circ$ was 1.2 eV. This result did not show a large discrepancy with the aforementioned result obtained by the conventional method. Therefore, the conventional method appeared to be appropriate here.

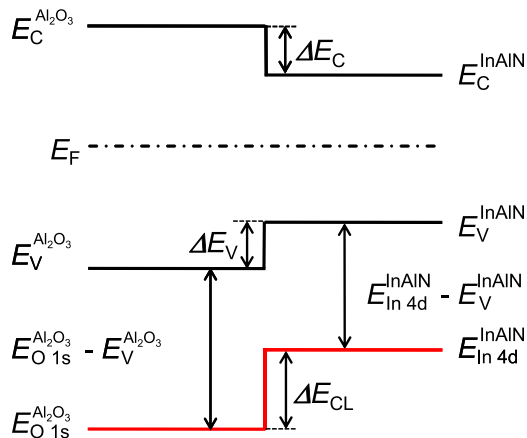


FIG. 2. Schematic diagram of the conventional method used to measure ΔE_V .

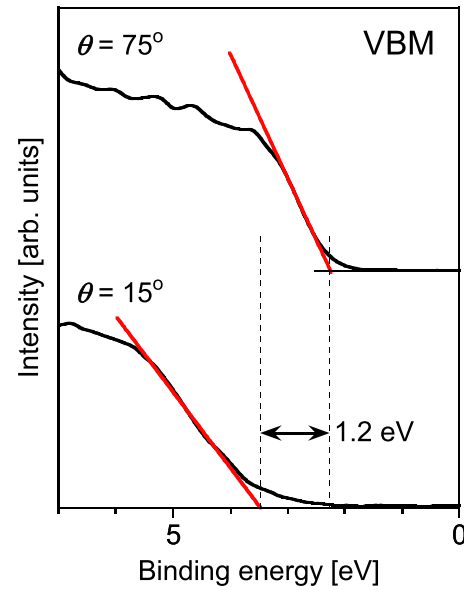


FIG. 3. VBM spectra observed for Al₂O₃ (2 nm)/InAlN interface at $\theta = 15^\circ$ and $\theta = 75^\circ$.

However, we found an anomalous phenomenon in the Al₂O₃ (2 nm)/In_{0.17}Al_{0.83}N/GaN structure. As θ increased, $E_{O1s_I}^{Al_2O_3}$ decreased, whereas E_{In4d}^{InAlN} increased. As a result, the energy difference ΔE_{CL} increased as θ decreased. The results are summarized in Table I. As can be seen, the difference between ΔE_{CL} at $\theta = 15^\circ$ and $\theta = 75^\circ$ was as large as 0.3 eV, considerably larger than the experimental error of ± 0.1 eV. This difference should not have been observed since the magnitude of ΔE_V was constant and independent of θ . In addition, the measured full width at half maximum (FWHM) of the In 4d spectra increased as θ increased, though that of O 1s_I did not increase markedly. The behavior of the core level spectra is also plotted in Fig. 4, where the measured binding energy and FWHM values are respectively indicated by open circles and rectangles vs. θ (the meaning of the solid lines will be described later). These results indicated that it was necessary to apply the conventional method carefully to the present structure.

As we reported previously,^{9,10} an abrupt internal potential gradient should have existed in the InAlN layer owing to its large spontaneous polarization. An internal potential gradient can be caused by the surface/interface charge generated by the difference in polarization and by surface/interface states. Therefore, there is a possibility that the potential gradient exists also in the Al₂O₃ layer on InAlN. Thus, correction of the measured ΔE_{CL} value is necessary. For the correction, we numerically calculated the effect of the internal potential gradient on the core-level spectra, to obtain the dependence of apparent binding energy and FWHM values on θ . Details of the principle and calculation method have

TABLE I. Results of angle-resolved XPS to measure ΔE_{CL} .

θ	$E_{O1s_I}^{Al_2O_3}$ (eV)	E_{In4d}^{InAlN} (eV)	ΔE_{CL} (eV)
15°	531.40	17.90	513.50
45°	531.28	18.01	513.27
75°	531.32	18.08	513.24

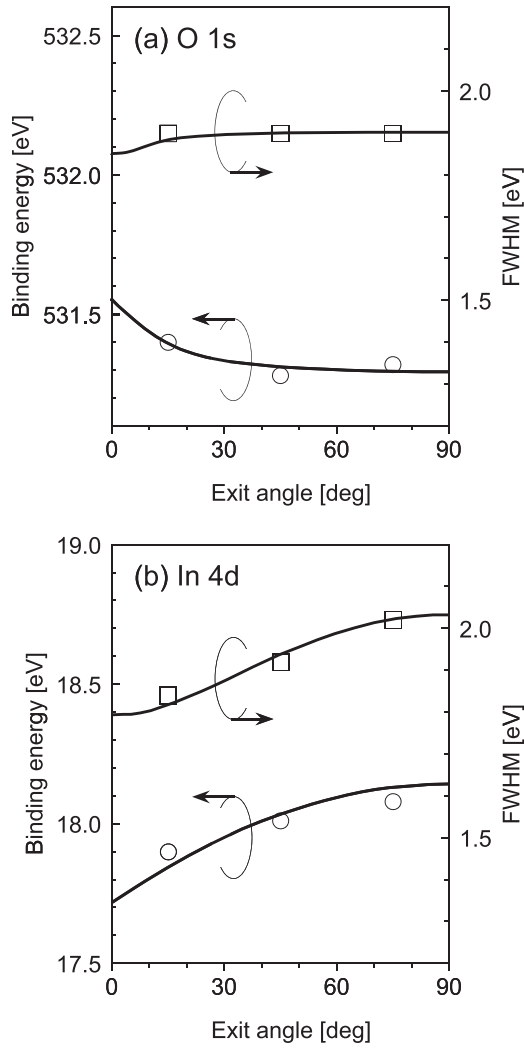


FIG. 4. Measured (open circles and rectangles) and simulated (solid lines) binding energy and FWHM vs. θ for (a) O 1s from the 2-nm-thick Al_2O_3 layer and (b) In 4d from the host InAlN layer.

been reported previously.¹⁰ Briefly, a core-level spectrum as a function of the binding energy, E , for a layer of thickness d can be given by

$$I(E) = \int_0^d I_0(E, z) \exp\left(-\frac{z}{\lambda}\right) dz, \quad (3)$$

where z is the depth from the surface and $I_0(E, z)$ denotes the spectrum generated at each depth. Here, $I_0(E, z)$ for a single spin orbital is represented by the pseudo-Voigt function. To estimate λ at each θ , λ_0 in Eq. (1) was calculated according to the previously reported theory.¹¹ When surface internal potential gradient is not negligible relative to λ , the z -dependence of the core-level energy should be taken into account in $I_0(E, z)$.

In this case, the assumption of opposite potential gradients in the Al_2O_3 and InAlN layers, as shown in Fig. 5, can explain the observed phenomena. The core levels are also inclined parallel to the VBM gradient. The calculation results used to fit the apparent binding energy and FWHM, assuming the internal potential drop to be -600 meV for 2-nm-thick Al_2O_3 layer and 2.5 eV in the opposite direction for the 15-nm-thick InAlN layer, are shown in Fig. 4 by the solid

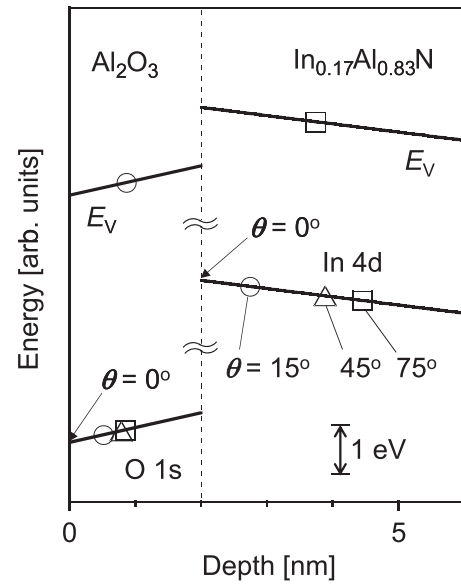


FIG. 5. Depth profiles for E_V , O 1s, and In 4d levels assumed in the calculation used to reproduce the observed phenomena. Open circles, triangles, and rectangles indicate the calculated apparent binding energy positions at $\theta = 15^\circ, 45^\circ$, and 75° , respectively.

lines (here the sign of the potential drop is defined to be positive when the potential goes down as the depth increases). The calculated results explained the behavior of apparent binding energy and FWHM depending on θ . As shown in Fig. 6, the apparent values of ΔE_{CL} obtained by experiment and by calculation assuming the potential gradient described above are in good agreement. However, these values are still apparent ones. As is shown in Fig. 5, the apparent ΔE_{CL} at $\theta = 0^\circ$ gives the difference between the core-level values at the top point of each layer. Therefore, to obtain the actual ΔE_{CL} at the $\text{Al}_2\text{O}_3/\text{InAlN}$ interface, we have to include the total potential drop in the Al_2O_3 layer, $\Delta V_{\text{Al}_2\text{O}_3}$ as follows:

$$\Delta E_{CL} = (E_{O1s}^{\text{Al}_2\text{O}_3} - E_{In4d}^{\text{InAlN}})_{\theta=0} + q\Delta V_{\text{Al}_2\text{O}_3}, \quad (4)$$

where q is the elementary charge. In this way, the actual core-level separation at the interface was derived to be 513.2 eV, which is also indicated in Fig. 6. Therefore, ΔE_V was found to be 1.2 eV.

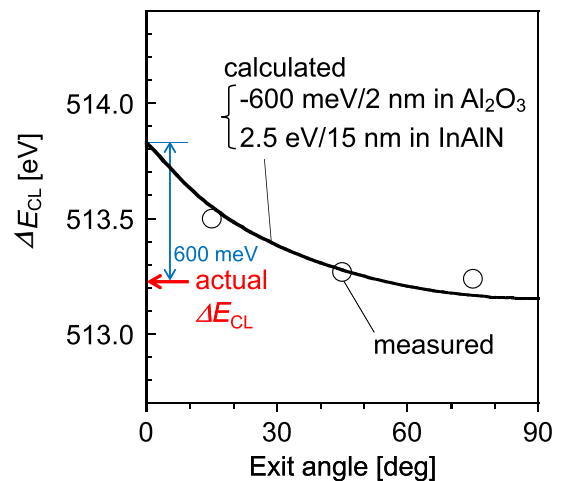


FIG. 6. Measured (open circles) and calculated (solid line) results for apparent ΔE_{CL} vs. θ .

In Fig. 5, the calculated apparent energy points, which should have been measured by XPS, for the core levels and the VBM are also indicated by open circles for $\theta = 15^\circ$, open triangles for $\theta = 45^\circ$, and open rectangles for $\theta = 75^\circ$. As θ increases, a deeper point should be probed according to Eq. (1). However, it should be noted that the depth corresponding to the apparent binding energy is not necessarily proportional to λ , owing to the modification of the spectral shapes as a result of integration of Eq. (3). Especially, the VBM is given by the edge of calculated spectra, while the positions of core-level spectra are extracted by the half-maximum center. Using these calculated points, it can be concluded that the observed apparent difference in the VBM between $\theta = 15^\circ$ and $\theta = 75^\circ$ in Fig. 3 should be close to the actual value because the internal potential gradient in the Al_2O_3 and InAlN layers is in opposite directions. Therefore, it is possible that the difference in VBM between $\theta = 15^\circ$ and $\theta = 75^\circ$ results in the same value as the actual ΔE_V .

Consequently, the conventional method provided a reasonable value of ΔE_V within the experimental error of ± 0.1 eV. Considering the experimental error for all the present results, it is safely concluded that the value of ΔE_V should be 1.2 ± 0.2 eV. Since the band gap of Al_2O_3 and InAlN has been, respectively, measured to be 6.7–7.0 eV (Refs. 12–15) and 4.6 eV,¹⁶ ΔE_C is estimated to be approximately 1 eV. This value appears to be sufficiently large to justify using an Al_2O_3 layer in combination with an InAlN layer to enhance the barrier function for a 2DEG at an InAlN/GaN heterointerface.

This work was supported by JSPS KAKENHI (Grant No. 24560022). The authors are thankful to Professor T. Hashizume for his encouragement and enlightening discussion.

- ¹J. Kuzmík, *IEEE Electron Device Lett.* **22**, 510 (2001).
- ²M. Higashiwaki and T. Matsui, *Jpn. J. Appl. Phys.* **43**, L768 (2004).
- ³O. Ambacher, R. Dimitrov, M. Stutzmann, B. E. Foutz, M. J. Murphy, J. A. Smart, J. R. Shealy, N. G. Weimann, K. Chu, M. Chumbes, B. Green, A. J. Sierakowski, W. J. Schaff, and L. F. Eastman, *Phys. Status Solidi B* **216**, 381 (1999).
- ⁴G. Pozzovivo *et al.*, *Appl. Phys. Lett.* **91**, 043509 (2007).
- ⁵K. Čičo, K. Hušeková, M. Ľapajna, D. Gregušová, R. Stoklas, J. Kuzmík, J.-F. Carlin, N. Grandjean, D. Pogany, and K. Fröhlich, *J. Vac. Sci. Technol. B* **29**, 01A808 (2011).
- ⁶O. Renault, L. G. Gosset, D. Rouchon, and A. Ermolieff, *J. Vac. Sci. Technol. A* **20**, 1867 (2002).
- ⁷M. R. Alexander, G. E. Thompson, and G. Beamson, *Surf. Interface Anal.* **29**, 468 (2000).
- ⁸J. R. Waldrop and R. W. Grant, *Appl. Phys. Lett.* **68**, 2879 (1996).
- ⁹M. Akazawa, T. Matsuyama, T. Hashizume, M. Hiroki, S. Yamahata, and N. Shigekawa, *Appl. Phys. Lett.* **96**, 132104 (2010).
- ¹⁰M. Akazawa, B. Gao, T. Hashizume, M. Hiroki, S. Yamahata, and N. Shigekawa, *J. Appl. Phys.* **109**, 013703 (2011).
- ¹¹S. Tanuma, C. J. Powell, and D. R. Penn, *Surf. Interface Anal.* **21**, 165 (1994).
- ¹²S. Miyazaki, *J. Vac. Sci. Technol. B* **19**, 2212 (2001).
- ¹³C. M. Tanner, Y. C. Perng, C. Frewin, S. E. Saddow, and J. P. Chang, *Appl. Phys. Lett.* **91**, 203510 (2007).
- ¹⁴M. L. Huang, Y. C. Chang, Y. H. Chang, T. D. Lin, J. Kwo, and M. Hong, *Appl. Phys. Lett.* **94**, 052106 (2009).
- ¹⁵Y. Hori, C. Mizue, and T. Hashizume, *Jpn. J. Appl. Phys.* **49**, 080201 (2010).
- ¹⁶R. E. Jones, R. Broesler, K. M. Yu, J. W. Ager III, E. E. Haller, W. Walukiewicz, X. Chen, and W. J. Schaff, *J. Appl. Phys.* **104**, 123501 (2008).